

Correlation Between Vortex Strength and Axial Velocity in a Trailing Vortex

Elgin A. Anderson* and Todd A. Lawton†
Utah State University, Logan Utah 84322-4130

The vortices that trail from the wingtips of a large aircraft provide a significant hazard to an aircraft that follows in its wake. The objective is to contribute to the understanding of these vortices by identifying the conditions where an axial velocity in excess of the freestream value will be generated in the core of a trailing vortex. The axial velocity near the core of a trailing vortex was measured using a triple-sensor hot-wire probe and compared with measured values of vortex circulation strength. The vortex was generated in a wind tunnel using a NACA 0015 wing model with a semispan aspect ratio of 0.80. A linear relationship between the axial velocity and a nondimensional circulation parameter is indicated. For small values of the circulation parameter, the axial velocity shows a velocity deficit. An increase in circulation strength results in a progressive increase in axial velocity, which can exceed the freestream velocity by as much as 70%. The results indicate that the magnitude of the axial velocity is sensitive to the two end-cap configurations, flat and rounded, that were tested. It was found that scaling the circulation parameter by the vortex radius collapses the data from both configurations to a single linear curve.

Nomenclature

b	= wing span
C	= constant equal to $(2\pi)^{-1}$ times the circulation
c	= wing chord
d	= vortex diameter
U	= freestream velocity
u, v, w	= local velocity in Cartesian coordinates
u_x, u_θ, u_r	= local velocity in cylindrical coordinates
x, θ, r	= cylindrical coordinates
α	= angle of attack
Γ	= circulation
ΔH	= head loss parameter

Introduction

It was suggested by Batchelor¹ that axial flow should occur inside a trailing line vortex and that it can be less than (deficit) or greater than (excess) the freestream velocity. His conclusion was based on an analysis of the equations of motion with axisymmetric line vortex assumptions. The following result was derived:

$$u_x^2 = U^2 + \int_r^\infty \frac{1}{r^2} \frac{\partial C^2}{\partial r} dr - 2\Delta H \quad (1)$$

where the dependent variable $C = ru_\theta$ represents $(2\pi)^{-1}$ times the circulation around a symmetrically placed circle, u_x is the axial velocity in the vortex core, and ΔH is an arbitrary function added by Batchelor to account for dissipation along a streamline passing through a viscous region of the flow, for example, the wing boundary layer. This result was obtained by equating the pressure terms from the radial momentum equation (integrated over the radial coordinate with axisymmetric trailing vortex assumptions) and Bernoulli's constant (including ΔH) applied between the freestream and a point near the center of the vortex. Equation (1) shows that an excess or deficit of the axial velocity will depend on a balance between the

overall dissipation term and the radial circulation gradient. If one assumes that the dissipation term and the vortex core radius remain relatively constant and that there is a monotonic increase in circulation away from the vortex center, then the axial velocity excess would increase as the overall circulation strength of the vortex is increased. In subsequent experimental studies, investigators have measured both types of axial velocity behavior and the results agree qualitatively with Batchelor's conclusion.

Two recent experimental studies performed by Chow et al.² and Devenport et al.³ provide examples of velocity excess and deficit behavior. Chow et al.² used a NACA 0012 rectangular wing section with a rounded end cap and a semispan aspect ratio of 0.75. The wing section was positioned at an angle of attack of $\alpha = 10$ deg while measurements were taken at approximately 0.16 to 0.67 chord lengths downstream of the wing. All measurement locations indicated an axial velocity excess of approximately $1.7U$, which decayed only slightly from the trailing edge to $0.67c$. Devenport et al.³ performed a similar study using a NACA 0012 rectangular wing section with a flat end cap, aspect ratio of 4.33, and $\alpha = 5$ deg. Velocity measurements taken at locations between 5 and 30 chord lengths behind the wing's trailing edge showed a deficit profile of approximately $0.84U$, which remained relatively constant over the downstream distance surveyed. Hence, both axial velocity excess and deficit in a trailing vortex can be confirmed by experiment, a result which supports Batchelor's early analysis. Later analyses by Green⁴ and Saffman⁵ provided additional theoretical support for these experimental observations.

Spalart⁶ provides insight to the axial velocity behavior. He supplements Batchelor's analysis by rationalizing a proportional relationship between the axial velocity and a nondimensional quantity defined here as the circulation parameter $\Gamma/(Ub)$, where Γ is the measured circulation strength and b is twice the model semispan. When this parameter was used, the differences between several experimental studies were reconciled. The data of Chow et al.,² which show an excess axial velocity of $1.78U$, give a circulation parameter value of 0.20. In contrast, Devenport et al.,³ reported a deficit profile that corresponds to a much lower circulation parameter of 0.028. Other investigations by Ramaprian and Zheng⁷ and McAlister and Takahashi⁸ showed that when the wing loading is low a deficit profile is detected. For larger wing loading, McAlister and Takahashi, Chigier and Corsiglia,⁹ and Dacles-Mariani et al.¹⁰ show that an excess profile is observed.

To evaluate the influence of the wing end-cap treatment, one must consider the differences in the near-field vortex structure for each configuration. Numerical predictions by Khorrami et al.¹¹ indicate the formation of multiple vortex structures produced as the vortex

Received 8 December 2001; revision received 13 February 2003; accepted for publication 15 February 2003. Copyright © 2003 by the American Institute of Aeronautics and Astronautics, Inc. All rights reserved. Copies of this paper may be made for personal or internal use, on condition that the copier pay the \$10.00 per-copy fee to the Copyright Clearance Center, Inc., 222 Rosewood Drive, Danvers, MA 01923; include the code 0021-8669/03 \$10.00 in correspondence with the CCC.

*Assistant Professor, Mechanical and Aerospace Engineering Department, Senior Member AIAA.

†Graduate Student, Mechanical and Aerospace Engineering Department.

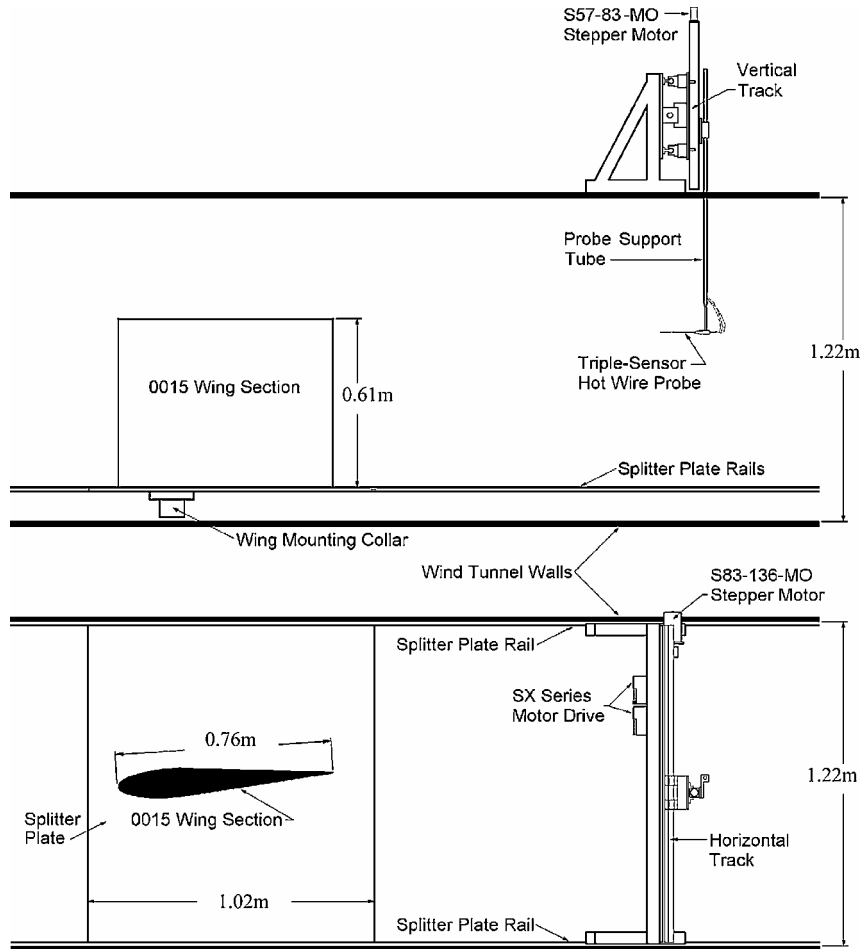


Fig. 1 Schematic views of the wind-tunnel test section arrangement for the experiments.

sheet is divided into segments at the abrupt edge of the flat end cap. In comparison, numerical predictions for rounded end-cap flow, Hsiao and Pauley,¹² Srinivasan and McCroskey,¹³ and Srinivasan et al.¹⁴ point to the smooth rollup of a single vortex sheet in the near field. The experimental measurements of McAlister and Takahashi⁸ reveal that at a given streamwise location the vortex formed from a wing with a flat end cap has a larger diameter and decreased axial velocity relative to the vortex formed by rounded end cap. Thus, it is deduced that for a given circulation strength a smaller vortex diameter is produced by the rounded end-cap configuration.

Experimental Arrangement and Procedure

In the present study, experimental data were obtained to gain further insight into the axial velocity behavior in the trailing vortex. The experiments were conducted in the low-speed wind tunnel at Utah State University's Aerodynamics Research Laboratory. The tunnel is an indraft type with a 1.2 by 1.2 m test section and an inlet contraction ratio of 9:1. The maximum tunnel velocity used in the current study was 30 m/s with a corresponding turbulence intensity of less than 0.5%. Three chord-based Reynolds numbers were investigated, 0.75×10^6 , 1×10^6 , and 1.25×10^6 , in the current work.

The NACA 0015 wing model had a 0.762-m chord and semispan of 0.610 m, which gave a semispan aspect ratio of 0.80. A band of 15 chordwise pressure ports located approximately at midsemispan were used to determine the zero-angle-of-attack position. The wing was mounted vertically on a splitter plate positioned 10 cm above the tunnel floor and could be rotated about its quarter-chord axis. The flat wingtip geometry could be modified by attaching a removable rounded end cap with a circular cross section.

Velocity measurements were obtained using an Auspex model AVEP-3-102 triple-sensor hot-wire probe operated by a TSI IFA300

constant temperature anemometer system. The hot-wire calibration was made using a TSI Model 1129 automatic velocity calibrator. A two-degree-of-freedom computer-controlled traverse with an accuracy of ± 0.01 mm in the transverse direction and ± 0.02 mm in the spanwise direction was used to position the probe. Streamwise traverse was accomplished by manually sliding the splitter plate along channels that extend along the length of the test section. The experimental arrangement is shown in Fig. 1.

Experimental Uncertainties

The local mean velocity results presented in this study are based on a time average of 2048 samples per data point acquired at a sample rate of 2000 Hz for a total sample period of 1.024 s. The sample period was defined by the minimum beyond which the mean quantities remained repeatable. Calibration of the hot-wire probe was accomplished using 17 points to cover a velocity range of 0–50 m/s. The maximum velocity measured in the test was approximately 30 m/s. The mean standard errors of the streamwise velocity calibration are as follows: less than 3% for velocities between 0 and 3 m/s, less than 2% for velocities between 3 and 16 m/s, and less than 0.1% for velocities greater than 16 m/s. The triple-sensor probe was calibrated over a pitch and yaw angle range of ± 30 deg using 5-deg increments. Conversion of raw voltage data to velocity components was accomplished using the method of Lekakis et al.¹⁵ Flow angles were resolved to an accuracy of ± 2 deg over the data range based on calibration check runs. Flow angularity in the flowfield did not exceed the angle limitations of the sensor. Vortex circulation strength was calculated by integration of the tangential velocity components along a square path surrounding the vortex. The length dimension of the square was 15.24 cm, and the measurement increment was 0.51 cm. Changing the length dimension of the square integration path by ± 2.54 cm produced less than a 0.5% change in

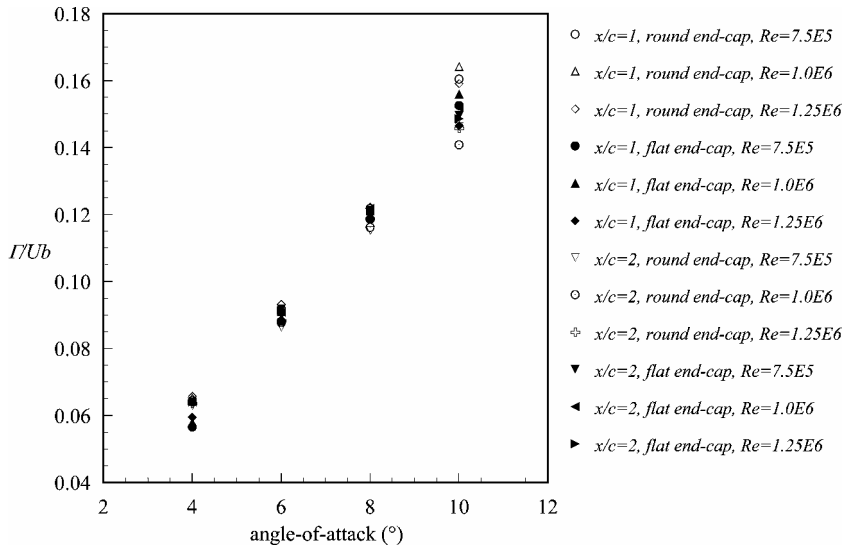


Fig. 2 Circulation parameter as a function of angle of attack: flat and rounded end-cap data are represented by solid and open symbols, respectively.

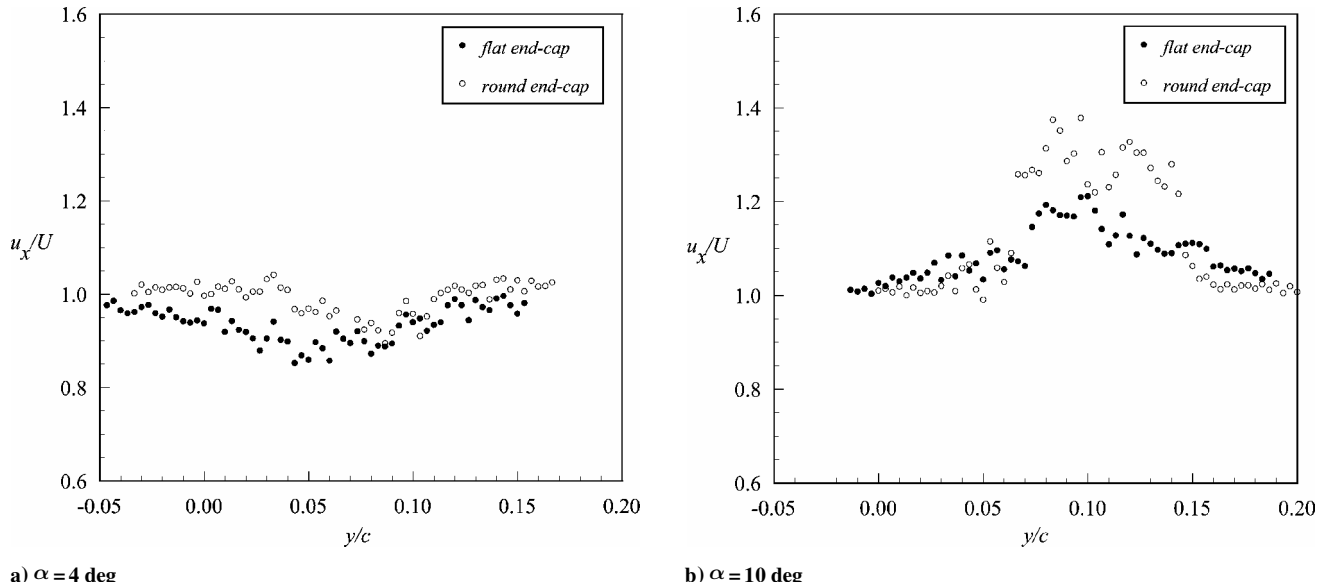


Fig. 3 Axial velocity profiles at $x/c = 2$.

the circulation value calculated with the flat end cap at $\alpha = 10$ deg and $x/c = 2$. All mean velocity data are normalized by the tunnel freestream velocity calculated from pitot-static tube dynamic pressure measurements that were simultaneously made with the hot-wire measurements. The Reynolds number was calculated using ambient temperature and pressure data acquired simultaneous with the dynamic pressure. The Reynolds number drifted by no more than ± 1000 from the nominal value over the duration of each flowfield survey due to ambient temperature changes.

Results

Vortex circulation values were calculated from an integration of the velocity field along a path that surrounded the vortex. The results are shown in terms of the nondimensional circulation parameter as a function of the wing angle of attack for three Reynolds numbers and two streamwise locations in Fig. 2. The difference in measured circulation strength between the $x/c = 1$ and $x/c = 2$ locations was relatively minor, indicating that the integration path contained nearly all of the shed vorticity. There was an increase in the scatter of the data at $\alpha = 10$ deg, which may be attributed to the onset of flow separation. The measurements obtained for $\alpha = 12$ deg showed significantly reduced circulation values consistent with separation.

Prandtl's lifting-line theory equates the circulation strength of a single trailing vortex to the strength produced by the bound vorticity at the wing root. For a fixed-geometry wing, the root circulation strength will increase in direct proportion to the lift produced. This result is consistent with the linear trend observed in Fig. 2. The circulation parameter values are seen to be relatively insensitive to end-cap treatment. Although it is expected that the rounded end cap produces lift more efficiently, this is not reflected in the strength of the trailing vortex but in the value of the proportionality constant that relates the vortex circulation strength to the wing lift.

The velocity profiles (Figs. 3a and 3b), show an axial velocity deficit for the lower wing loading ($\alpha = 4$ deg) and an excess for the higher wing loading ($\alpha = 10$ deg). The effect of the rounded end cap is to produce a greater axial velocity in the vortex compared to that generated by flat end cap. A relatively large scatter in the data is observed in the axial velocity that prevented a representative value u_x from being defined based strictly on the radial coordinate. Therefore, in the present work, u_x is defined as follows: For velocity excess, u_x is equal to the maximum velocity recorded near the vortex center, and for velocity deficit, u_x is equal to the minimum velocity recorded near the vortex center. The axial velocity values are shown for all tested configurations as a function of angle of attack in Fig. 4.

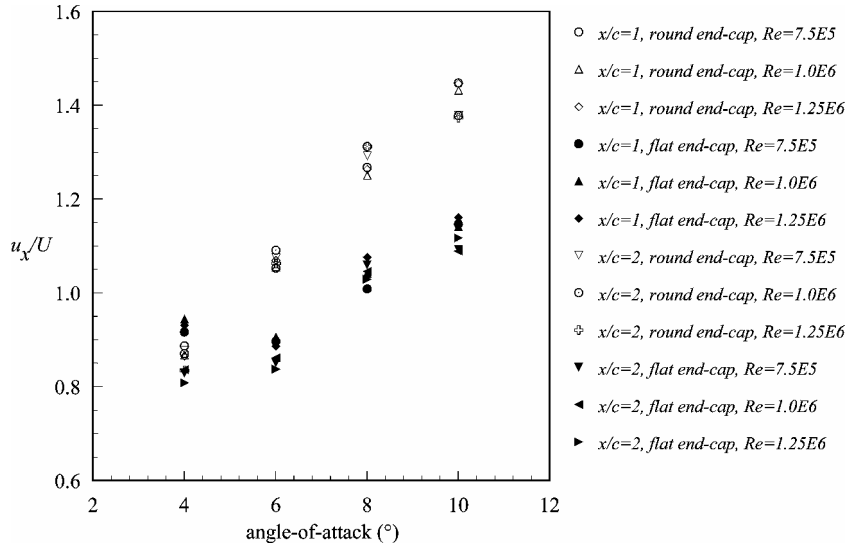


Fig. 4 Axial velocity magnitude as a function of angle of attack.

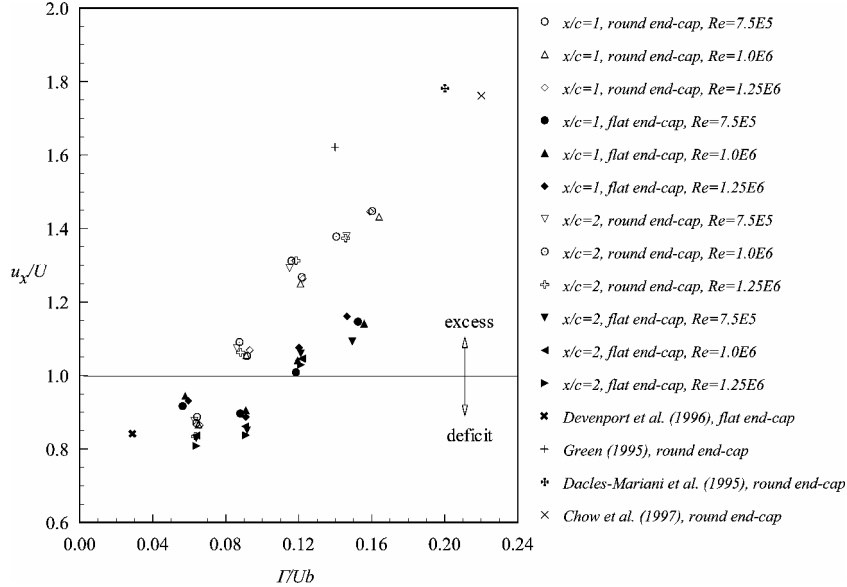


Fig. 5 Axial velocity near the center of the vortex as a function of circulation parameter.

A linear increase in axial velocity with respect to angle of attack is apparent for both end-cap configurations, although the magnitude is noticeably larger for the rounded end cap. Results for the flat end-cap configuration at lower wing loading ($\alpha = 4$ deg) indicate a significant deviation from the linear trend, as well as a sensitivity to streamwise measurement location. In contrast, the linear relationship is accurate for the rounded end-cap data over all wing angles of attack. The fact that axial velocity deficit values less than $0.8U$ are not observed and that the linear trend appears only valid above $0.9U$ may point to a minimum deficit limit in the wing wake.

A comparison between the vortex circulation parameter and axial velocity from the current study as well as from several other investigations is presented in Fig. 5. A linear trend is clearly observed in the present data, and they correlate well with the independent results. Also seen is the significant effect of the end-cap geometry on the axial velocity with the lower velocity corresponding to the flat end-cap configuration. The difference in axial velocity magnitude is linked to a contrast in vortex circulation density between the two end-cap configurations. For the rounded end cap, the flow separation is determined by the local pressure field that develops as fluid moves in a smooth manner around the wingtip. In contrast, the flow separation at the flat end cap is determined by the presence of the sharp edge, which forces the boundary layer to separate at fixed locations. Pre-

vious experimental⁸ and computational^{11–14} results indicate that for a given circulation strength a smaller vortex diameter is produced by the rounded end-cap configuration. Although a vortex produced by either the flat or the rounded end cap has a comparable circulation, the vortex produced by the rounded end cap has a smaller diameter and, therefore, has a higher circulation density. According to Batchelor,¹ the magnitude of the axial velocity in a trailing vortex is determined by a balance between the energy loss due to dissipation in the wing boundary layer and the radial gradient in circulation strength. If we assume that the viscous dissipation and the circulation is the same for both configurations, then the rounded end cap, which produces a smaller more concentrated vortex, has a larger radial gradient in circulation strength. This result applied to Batchelor's theory also predicts that the rounded end cap will generate the larger axial velocity.

The sensitivity of the axial velocity and vortex diameter to end-cap configurations indicates that the diameter is an important scaling parameter for the circulation strength. In Figs. 6a–6c, transverse velocity profiles for the flat and rounded end-cap configurations are compared at $x/c = 1$ and 2 and for $\alpha = 4$ and 10 deg. Those configurations are representative of the general effect of end-cap geometry on vortex diameter. From each profile, the vortex diameter was estimated and is noted on Fig. 6. Although the estimate is somewhat

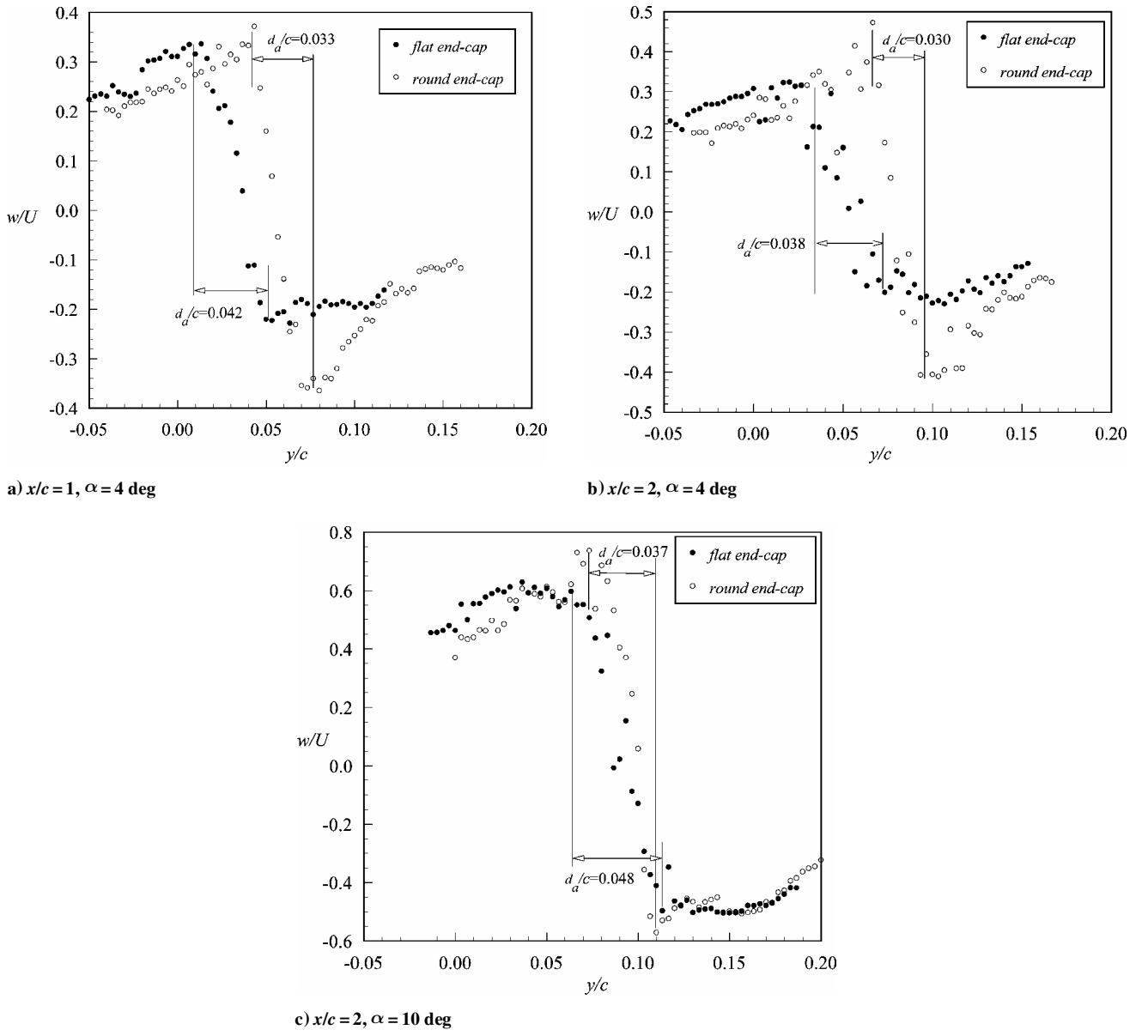


Fig. 6 Vortex transverse velocity profiles.

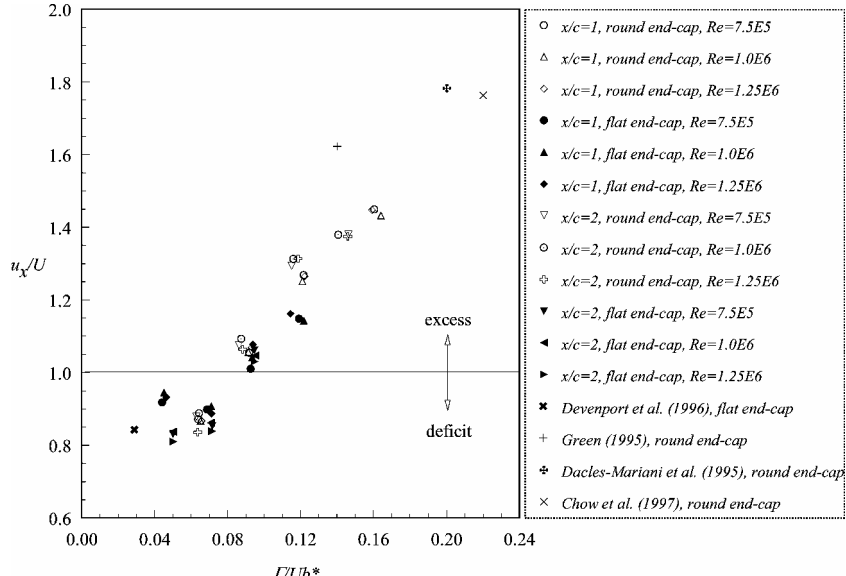


Fig. 7 Axial velocity near the center of the vortex as a function of modified circulation parameter.

subjective, the trend of smaller diameter for the rounded end cap is apparent and consistent with results from other investigations (e.g., McAlister and Takahashi⁸). For a given Reynolds number, angle of attack, and streamwise measurement location, the trailing vortex generated with the rounded end cap produced a smaller radius than that produced with the flat end cap. The results are consistent for both velocity excess and deficit conditions. The average ratio of vortex diameter from the flat end-cap to vortex diameter from the rounded end cap calculated from the profiles is approximately 1.28. This ratio was then used to scale the circulation parameter for the flat end-cap data to define a modified circulation parameter,

$$\begin{aligned} \Gamma/Ub^* &= \Gamma_{\text{round}}/Ub = (\Gamma_{\text{flat}}/Ub) \overline{(d_a \text{ round}/d_a \text{ flat})} \\ &= (\Gamma_{\text{flat}}/Ub)(1/1.28) \end{aligned} \quad (2)$$

In Fig. 7, the results from this scaling are presented. The scaling of the flat end-cap circulation parameter by the diameter ratio brings the two linear trends into close agreement. It is expected that this result is valid, not only for variations in end-cap treatment, but also for any other variations in wing geometry, for example, sweep, taper, and section shape, that affect the vortex diameter.

Conclusions

The axial velocity near the center of a trailing vortex was measured using a triple-sensor hot-wire probe and compared to the vortex circulation strength calculated by integration of the transverse velocity components around a path surrounding the vortex. From the results presented here, it is shown that a linear relationship between the circulation strength and wing angle of attack exists that is consistent with Prandtl's lifting-line theory. It is also shown that a linear relationship exists between the axial velocity within the core of a trailing vortex and the wing's angle of attack. For the current investigation, this linear trend is valid for cases where the axial velocity was greater than 90% of the freestream velocity. Below the 90% threshold value, there is a deviation from this linear trend that suggests the presence of a maximum deficit limit for trailing vortices.

The axial velocity and the circulation parameter are shown to be linearly proportional to the angle of attack of the wing and, therefore, are proportional to each other. This proportionality is predicted by Batchelor's theory¹ for the axial velocity if one assumes that the changes in the vortex radius and the viscous dissipation on the wing with respect to angle of attack are negligible. The slope of the linear relationship is comparable for the two end-cap configurations. However, the vortex generated by the rounded end cap produces a higher axial velocity at a given circulation parameter value.

It was shown that the end-cap geometry has a significant effect on the magnitude of the axial velocity excess. At a given angle of attack, the vortex produced from a rounded end cap generates a larger axial velocity and has a smaller diameter than that produced from a flat end cap. Because the measured circulation strengths are comparable between the two configurations, it is concluded that the larger axial velocity generated from the rounded end cap is caused

by a larger radial circulation gradient. Again, this conclusion is motivated by the theoretical analysis of Batchelor¹ that predicts such a relationship between the two parameters.

An important scaling parameter for this problem is shown to be the vortex diameter. Scaling the circulation parameter by the ratio of vortex diameter for the flat and rounded end-cap configurations allows the relationship between axial velocity and circulation parameter to be approximated by a single line. The results from previous investigations are shown to correlate well with the current study.

Acknowledgment

The authors gratefully acknowledge financial support from NASA Langley Research Center under Grant NAG-1-1999 during the course of this investigation.

References

- Batchelor, G. K., "Axial Flow in Trailing Line Vortices," *Journal of Fluid Mechanics*, Vol. 20, 1964, pp. 645-658.
- Chow, J. S., Zilliac, G. G., and Bradshaw, P., "Mean and Turbulence Measurements in the Near Field of a Wingtip Vortex," *AIAA Journal*, Vol. 35, No. 10, 1997, pp. 1561-1567.
- Devenport, W. J., Rife, M. C., Liapis, S. I., and Follin, G. J., "The Structure and Development of a Wing-Tip Vortex," *Journal of Fluid Mechanics*, Vol. 312, 1996, pp. 67-106.
- Green, S. I., "Wing Tip Vortices," *Fluid Vortices*, edited by S. I. Green, Kluwer Academic, Dordrecht, The Netherlands, 1995, Chap. 10.
- Saffman, P. G., *Vortex Dynamics*, Cambridge Monographs on Mechanics and Applied Mathematics, Cambridge Univ. Press, Cambridge, UK, 1992, pp. 257-264.
- Spalart, P. R., "Airplane Trailing Vortices," *Annual Review of Fluid Mechanics*, Vol. 30, 1998, pp. 107-138.
- Ramaprian, B. R., and Zheng, Y., "Measurements in Rollup Region of the Tip Vortex from a Rectangular Wing," *AIAA Journal*, Vol. 35, No. 12, 1997, pp. 1837-1843.
- McAlister, K. W., and Takahashi, R. K., "NACA 0015 Wing Pressure and Trailing Vortex Measurements," NASA TP 3151, Nov. 1991.
- Chigier, N. A., and Corsiglia, V. R., "Wind-Tunnel Studies of Wing Wake Turbulence," *Journal of Aircraft*, Vol. 9, No. 12, 1972, pp. 820-825.
- Dacles-Mariani, J., Zilliac, G. G., Chow, J. S., and Bradshaw, P., "Numerical/Experimental Study of a Wingtip Vortex in the Near Field," *AIAA Journal*, Vol. 33, No. 9, 1995, pp. 1561-1568.
- Khorrami, M. R., Singer, B. A., and Radeztsky, R. H., "Reynolds-Averaged Navier-Stokes Computations of a Flap-Side-Edge Flowfield," *AIAA Journal*, Vol. 37, No. 1, 1999, pp. 14-22.
- Hsiao, C.-T., and Pauley, L. L., "Numerical Study of the Steady-State Tip Vortex Flow Over a Finite-Span Hydrofoil," *Journal of Fluids Engineering*, Vol. 120, No. 2, 1998, pp. 345-353.
- Srinivasan, G. R., and McCroskey, W. J., "Navier-Stokes Calculations of Hovering Rotor Flowfields," *Journal of Aircraft*, Vol. 25, No. 10, 1988, pp. 865-874.
- Srinivasan, G. R., Baeder, J. D., Obayashi, S., and McCroskey, W. J., "Flowfield of a Lifting Rotor in Hover: A Navier-Stokes Simulation," *AIAA Journal*, Vol. 30, No. 10, 1992, pp. 2371-2378.
- Lekakis, I. C., Adrian, R. J., and Jones, B. G., "Measurement of Velocity Vectors with Orthogonal and Non-Orthogonal Triple-Sensor Probes," *Experiments in Fluids*, Vol. 7, 1989, pp. 228-240.